



This is a repository copy of *The extent of counterion dissociation at the interface of cationic diblock copolymer nanoparticles in non-polar solvents*.

White Rose Research Online URL for this paper:
<https://eprints.whiterose.ac.uk/161076/>

Version: Accepted Version

Article:

Smith, G.N., van Meurs, S. and Armes, S.P. orcid.org/0000-0002-8289-6351 (2020) The extent of counterion dissociation at the interface of cationic diblock copolymer nanoparticles in non-polar solvents. *Journal of Colloid and Interface Science*, 577. pp. 523-529. ISSN 0021-9797

<https://doi.org/10.1016/j.jcis.2020.04.102>

Article available under the terms of the CC-BY-NC-ND licence (<https://creativecommons.org/licenses/by-nc-nd/4.0/>).

Reuse

This article is distributed under the terms of the Creative Commons Attribution-NonCommercial-NoDerivs (CC BY-NC-ND) licence. This licence only allows you to download this work and share it with others as long as you credit the authors, but you can't change the article in any way or use it commercially. More information and the full terms of the licence here: <https://creativecommons.org/licenses/>

Takedown

If you consider content in White Rose Research Online to be in breach of UK law, please notify us by emailing eprints@whiterose.ac.uk including the URL of the record and the reason for the withdrawal request.



eprints@whiterose.ac.uk
<https://eprints.whiterose.ac.uk/>

The extent of counterion dissociation at the interface of cationic diblock copolymer nanoparticles in non-polar solvents

Gregory N. Smith^{a,b,*}, Sandra van Meurs^a, Steven P. Armes^a

^aDepartment of Chemistry, University of Sheffield, Brook Hill, Sheffield, South Yorkshire, S3 7HF, United Kingdom

^bNiels Bohr Institute, University of Copenhagen, H. C. Ørsted Institute, Universitetsparken 5, 2100 Copenhagen Ø, Denmark

Abstract

Hypothesis Diblock copolymer nanoparticles prepared in non-polar solvents that are sterically stabilized but possess ionic functionality from the inclusion of cationic comonomers in the stabilizer shell are known to exhibit complex electrokinetic behavior (Chem. Sci. 9 (2018) 922–934). For example, core-shell nanoparticles with cationic comonomers located solely within the shell layer have lower magnitude electrophoretic mobilities than nanoparticles containing the same cationic comonomers located within the core, and nanoparticles prepared using a minor fraction of steric stabilizer chains containing cationic comonomer repeat units have comparable electrophoretic mobilities to nanoparticles prepared with this cationic comonomer solely located within the core. We hypothesize that these observations can be explained in terms of the strength of the Coulombic interaction between counterions and the nanoparticle interface.

Experiments The highly-fluorinated anionic counterion associated with these cationic nanoparticles is studied by ¹⁹F nuclear magnetic resonance (NMR) spectroscopy in *n*-dodecane. This revealed only one type of ¹⁹F environment for a soluble macromolecular cation (the oil-soluble steric stabilizer chains used to prepare the nanoparticles), whereas two distinct environments were observed for the sterically-stabilized cationic nanoparticles. Both ¹⁹F diffusion NMR and ¹⁹F–¹³C heteronuclear single quantum correlation (HSQC) measurements support the existence of two environments for this counterion.

Findings The existence of two distinct ¹⁹F environments for the highly-fluorinated anion associated with the sterically-stabilized nanoparticles demonstrates the presence of spectroscopically distinguishable populations of ion pairs and of fully dissociated free anions. ¹⁹F NMR spectra recorded for sterically-stabilized nanoparticles with a fully ionic shell (all stabilizer chains containing the cationic comonomer) and those with a partly ionic shell (10% of stabilizer chains containing the cationic comonomer) reveal a higher proportion of dissociated anions in the partly ionic case. This suggests a stronger Coulombic interaction between counterions and the cationic interface when the shell is fully ionic, which accounts for the observed reduction in the magnitude of the electrophoretic mobility.

Keywords: Charged colloids, Nuclear magnetic resonance, Diffusion, Polymer self-assembly

1. Introduction

Producing and stabilizing ionic species in non-polar solvents (with a relative permittivity or dielectric constant, $\epsilon_r \approx 2$) is known to be experimentally challenging [1]. Typically, large molecules or self-assembled species are used to minimize the formation of ion pairs or higher-number ion aggregates [1–3]. Despite the difficulty in producing such charged species, they are essential for various technological applications, such

*Corresponding author

Email address: gregory.smith@nbi.ku.dk (Gregory N. Smith)

as petrochemicals, printing, electrorheological fluids, electrophoretic displays, or polymerization catalysis [4–11]). However, ion dissociation constants for electrolytes in low dielectric media are extremely low [12–14]. Moreover, the low relative permittivity has some interesting consequences for the nature of the charged species, such as triple-ion formation and counterion condensation [15–18].

10 Various types of organic molecules, such as self-assembled aggregates [2, 19, 20], weakly-coordinating ions [14, 21], dendrimers [3], or macromolecules [22], are often employed to stabilize ions in non-polar solvents. One advantage of such species is that they are potentially amenable to analysis by nuclear magnetic resonance (NMR) spectroscopy, using techniques that make use of the nuclear Overhauser effect to study cross-relaxation or field gradients to study diffusion [12, 23–27]. For example, diffusion NMR has proved to
15 be very useful for studying surfactants and polymers [28–32]. There are several reports of ion association and cluster formation with either small molecule electrolytes or polyelectrolytes [13, 22, 26, 27, 33, 34], and these are particularly relevant to this study of Coulombic interactions in low dielectric media. In non-polar solvents, ion pairs and higher-number aggregates are often observed, rather than fully dissociated free ions [24, 25]. Free ions must be present; electrolytic conductivity measurements would not be possible otherwise
20 [12–14]. Their concentration is vanishingly small in such systems, and this means that the identification of such species is challenging. As far as we are aware, only ion pairs and multiplets have been directly observed for low dielectric, aliphatic solvents [26, 27, 34]. Free ions have never been directly detected spectroscopically.

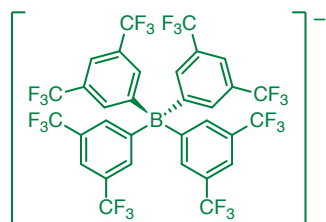
Sterically-stabilized diblock copolymer nanoparticles are prepared directly in *n*-dodecane using a technique known as polymerization-induced self-assembly (PISA) [35]. Steric stabilization is, in general, essential
25 to maintain the colloidal stability of nanoparticles in non-polar media. This is the case even for charged nanoparticles in non-polar solvents [18, 36, 37], despite some claims that there is an electrostatic (electrocratic) component to the stability of charged particles in non-polar solvents [38–41]. This is in contrast to water, where charge can be used to achieve colloidal stability [42–44]. We use *n*-dodecane as the continuous phase for this study, which has a relative permittivity (ϵ_r) of 2.01 at 25 °C [45]. The oil-insoluble, core-
30 forming block is poly(benzyl methacrylate) (PBzMA), while the cationic comonomer [(2-(methacryloyloxy)-ethyl)trimethylammonium]⁺ ([MOTMA]⁺) is statistically copolymerized with stearyl methacrylate (SMA) to form the charged oil-soluble steric stabilizer chains (see Figure 1). This counterion to this cationic comonomer is the weakly-coordinating, highly-fluorinated anion [tetrakis-3,5-bis(trifluoromethyl)phenyl]-
borate]⁻ ([TFPhB]⁻) that promotes charge formation in non-polar media. This is an approach that has
35 been used to produce charged nanoparticles in the literature previously [16, 18, 36, 46–48]. In addition, the [P(SMA-*stat*-MOTMA)⁺[TFPhB]⁻ stabilizer chains alone are used as a model oil-soluble polymeric species. This specific set of materials was selected due to a particularly surprising and, as of yet, unexplained observation relating to such charged shell nanoparticles in a salt-free, non-polar medium [18]. We previously
40 showed that the magnitude of the electrophoretic mobility of particles with charged shells is lower than that of ones with charged cores, even when the number of ionizable units in the polymer is the same. Intriguingly, when the amount of ionic stabilizer was reduced to \lesssim 30% (the remainder being nonionic), the particles had a higher magnitude electrophoretic mobility than particles where all the stabilizer was ionic [18, 48]. No existing electrokinetic theory can explain these observations.

Because of the high local density of ionic species at the interface and the low relative permittivity of the
45 medium, we hypothesize that these phenomena are due to the degree of Coulombic interaction at the interface between ionic moieties in the steric stabilizer and counterions. To characterize the Coulombic interaction between counterions and the colloid interface, we use ¹H, ¹³C, and ¹⁹F NMR spectroscopy. Specifically, ¹⁹F diffusion NMR and ¹⁹F–¹³C heteronuclear single quantum correlation (HSQC) measurements were performed to examine to what extent the highly-fluorinated anion exists as a free ion, as opposed to a paired ion.

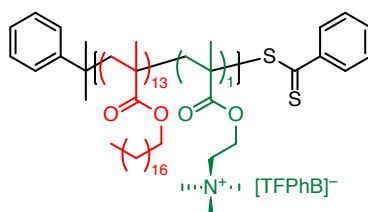
50 2. Experimental

2.1. Materials

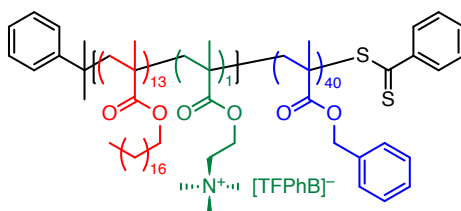
The synthesis of diblock copolymers and diblock copolymer nanoparticles was slightly modified from that reported in the literature for similar charged polymers [18], and further details are given in the Supporting Material. Figure 1(a) shows the structure of the highly-fluorinated, weakly-coordinating anion



(a) Tetrakis(3,5-bis(trifluoromethyl)phenyl)borate anion
([TFPhB]⁻)



(b) Poly(stearyl methacrylate-[2-(methacryloyloxy)ethyl] trimethylammonium) statistical copolymer
([P(SMA₁₃-stat-MOTMA₁)⁺[TFPhB]⁻] or [P(S₁₃-stat-M₁)⁺[TFPhB]⁻])



(c) P(SMA-*stat*-MOTMA)-poly(benzyl methacrylate) block copolymer
([P(SMA₁₃-*stat*-MOTMA₁)-PBzMA₄₀]⁺[TFPhB]⁻] or
[P(S₁₃-*stat*-M₁)-PB₄₀]⁺[TFPhB]⁻)

Figure 1: Chemical structures of the ionic species used in this study: (a) the [tetrakis[3,5-bis(trifluoromethyl)phenyl]borate]⁻ anion, (b) the cationic poly(stearyl methacrylate-[2-(methacryloyloxy)ethyl]trimethylammonium) statistical copolymer, which is also used as macromolecular chain-transfer agent for RAFT-mediated PISA [35], and (c) the cationic [P(SMA-*stat*-MOTMA)-poly(benzyl methacrylate)] diblock copolymer nanoparticles. The abbreviations used in subsequent legends are shown.

55 ([tetrakis[3,5-bis(trifluoromethyl)phenyl]borate]⁻, [TFPhB]⁻). The cationic poly(stearyl methacrylate-[2-(methacryloyloxy)ethyl]trimethylammonium) ([P(SMA₁₃-*stat*-MOTMA₁)⁺ [TFPhB]⁻ or [P(S₁₃-*stat*-M₁)⁺ [TFPhB]⁻) RAFT macromolecular chain-transfer agent (macro-CTA) is shown in Figure 1(b) and is studied both as a solution polymer and used as the steric stabilizer for the RAFT-mediated polymerization-induced self-assembly (PISA) [35] synthesis of the diblock copolymer nanoparticles. The structure of the
60 cationic diblock copolymer [P(SMA-*stat*-MOTMA)-poly(benzyl methacrylate)]⁺ [TFPhB]⁻ ([P(SMA₁₃-*stat*-MOTMA₁)-PBzMA₄₀]⁺ [TFPhB]⁻ or [P(S₁₃-*stat*-M₁)-PB₄₀]⁺ [TFPhB]⁻) that forms the nanoparticles is shown in Figure 1(c).

2.2. Nuclear magnetic resonance (NMR)

NMR (except HSQC) measurements were performed on a Bruker AVANCE III HD NMR spectrometer
65 operating at 500.13 MHz for ¹H (470.59 MHz for ¹⁹F) with a standard 5mm high resolution probehead (maximum gradient strength 50 G cm⁻¹). HSQC measurements were performed on a Bruker AVANCE III NMR spectrometer operating at 500.07 MHz for ¹H (470.54 MHz for ¹⁹F) equipped with a 5 mm QCI-F type CryoProbe. Spectra were referenced to lock solvent (toluene-*d*₈), which was introduced as a capillary insert.

70 Standard ¹H experiments were recorded using a 30° pulse for excitation, 64k acquisition points over a spectral window of 100 kHz with 16 transients and a relaxation delay of 1 s. For quantitative ¹⁹F experiments, the T1 relaxation times were first determined using an inversion recovery experiment. The ¹⁹F T1 times was determined to be ~ 750 ms for the nanoparticles. Quantitative ¹⁹F experiments were therefore recorded using a 90° pulse for excitation, a 46.875 kHz spectral window with 64k points. In each case 64 transients
75 were recorded with a 30 s relaxation delay between pulses. Peaks in the 1D quantitative ¹⁹F NMR spectra were fit as a sum of Lorentzian functions using the Fityk program [49].

Diffusion NMR measurements were performed using a stimulated echo with bipolar gradients (standard Bruker pulse sequence **stebpgp1s**), using a 16-step linear gradient ramp from 5% to 95% and values for diffusion time (Δ) and gradient pulse (δ) to obtain 90–95% signal attenuation at the highest gradient
80 strength. For ¹H diffusion NMR measurements, generally 16 transients per increment were used, whilst 128 scans per increment were used for ¹⁹F diffusion NMR measurements. Spectral windows for ¹H and ¹⁹F diffusion NMR measurements were 100 kHz and 23.4 kHz, using 32K and 46.8k points and relaxation delays of 3 s and 2 s, respectively. Diffusion NMR data were analyzed by producing DOSY plots in DOSY Toolbox 2.7 [50].

85 Heteronuclear single quantum correlation (HSQC) measurements were performed using acquisitions windows of 32.9 kHz and 20.7 KHz in ¹⁹F and ¹³C dimensions, respectively, using 4k acquisition points in the direct dimension and 8 transients for each of 256 increments in the indirect dimension.

3. Results and Discussion

The application of ionizable species in non-polar solvents requires their ability to acquire formal charge
90 (ion pair separation) and, in some situations, to respond to an applied electric field [4–11]. The low relative permittivity of non-polar hydrocarbon solvents means that Coulombic interactions are longer ranged and that the concentration of free ions is very low [12–14, 51]. This makes the detection of such species extremely challenging.

3.1. NMR spectroscopy of fully ionic macromolecules and nanoparticles

95 Clearly, the cationic species shown in Figure 1 are suited to analysis by ¹H and ¹³C NMR spectroscopy. Halogenated, and particularly fluorinated, anions increase the stability of ions in non-polar solvents [13, 14], and this means that the highly-fluorinated anion also shown in Figure 1 can also be readily detected by ¹⁹F NMR spectroscopy as well. Moreover, all the fluorine nuclei in this molecule are equivalent, which confers maximum sensitivity in ¹⁹F NMR spectra. In addition, two types of two-dimensional (2D) NMR
100 experiments were performed. ¹H and ¹⁹F diffusion NMR and ¹⁹F-¹³C correlation (HSQC) NMR experiments were performed to determine the self-diffusion coefficient and bond connectivity, respectively. Such

measurements are important to understand the origin of the 1D ^{19}F NMR peaks. Solutions of $[\text{P}(\text{SMA}_{13}\text{-stat-MOTMA}_1)]^+[\text{TFPhB}]^-$ (7 mol m^{-3}) and dispersions of $[\text{P}(\text{SMA}_{13}\text{-stat-MOTMA}_1)\text{-PBzMA}_{40}]^+[\text{TFPhB}]^-$ (volume fraction $\phi = 0.08$) were prepared in *n*-dodecane at the highest possible concentration in each case to enhance signal-to-noise.

^{19}F NMR spectra recorded for the $[\text{TFPhB}]^-$ anion associated with each of the cations examined in this study (see Figure 1) are shown in Figure 2. Since the highly-fluorinated anion is identical, the observed chemical shifts are very similar. One peak is observed at -62 ppm for $[\text{TFPhB}]^-$ associated with the oil-soluble $[\text{P}(\text{SMA}_{13}\text{-stat-MOTMA}_1)]^+$ copolymer. In contrast, the 1D ^{19}F NMR spectrum of the $[\text{TFPhB}]^-$ anion associated with the sterically-stabilized $[\text{P}(\text{SMA}_{13}\text{-stat-MOTMA}_1)\text{-PBzMA}_{40}]^+$ diblock copolymer nanoparticles is qualitatively different. Although located at essentially the same chemical shift as that of the copolymer cation, the primary ^{19}F peak is significantly broadened. (This would be expected for peaks in an NMR spectrum arising from a macromolecule [52].) A second, much less intense peak in the ^{19}F spectrum is now also discernible at approximately -63 ppm. Thus, there are two ^{19}F species in similar, yet locally distinct, environments in this case. We hypothesize that the major peak corresponds to anions that are tightly bound to the nanoparticle through Coulombic attraction. In contrast, the minor peak corresponds to free anions that are formally dissociated from the nanoparticles.

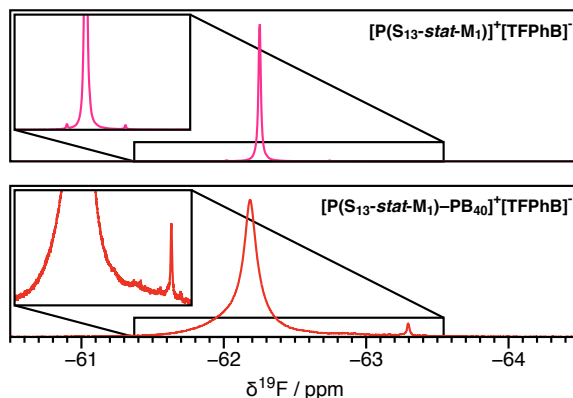


Figure 2: 1D ^{19}F NMR spectra recorded for the ionic species shown in Figure 1. Only one peak is observed for a solution of the $[\text{P}(\text{SMA}_{13}\text{-stat-MOTMA}_1)]^+[\text{TFPhB}]^-$ statistical copolymer dissolved in *n*-dodecane (7 mol m^{-3}). In contrast, two peaks are observed for dispersions of cationic $[\text{P}(\text{SMA}_{13}\text{-stat-MOTMA}_1)\text{-PBzMA}_{40}]^+[\text{TFPhB}]^-$ nanoparticles prepared in *n*-dodecane ($\phi = 0.08$). The insets show a magnified baseline.

Before analyzing this spectrum in detail, we consider other possible explanations for this minor peak. For example, it could be simply due to a fluorine-containing impurity within the sample. In principle, such an impurity could be present within the *n*-dodecane, but a 1D ^{19}F spectrum of this solvent contains no detectable ^{19}F peaks. Alternatively, such an impurity could be associated with the sterically-stabilized nanoparticles. However, there are no discernible ^{19}F peaks in a 1D spectrum of a dispersion of nonionic $\text{PSMA}_{13}\text{-PBzMA}_{40}$ nanoparticles, prepared under the same conditions as the cationic $[\text{P}(\text{SMA}_{13}\text{-stat-MOTMA}_1)\text{-PBzMA}_{40}]^+[\text{TFPhB}]^-$ nanoparticles except for the use of an ion-free PSMA_{13} homopolymer as the steric stabilizer block. (These ^{19}F NMR spectra are shown in Figure S1.) In principle, this minor peak might represent an impurity or other chemical environment associated with the $[\text{TFPhB}]^-$ anion. However, no corresponding peak is observed in the baseline of the 1D ^{19}F NMR spectrum of the oil-soluble cationic $[\text{P}(\text{SMA}_{13}\text{-stat-MOTMA}_1)]^+$ copolymer (see Figure 2).

Another possibility could be spin-spin coupling between the ^{19}F and ^{13}C nuclei, both with nuclear spin of $1/2$ [53]. Only $\sim 1\%$ of carbon nuclei are the ^{13}C isotope [54], but this is sufficient to result in detectable spin-spin coupling. The faint peak from $^{19}\text{F}\text{-}^{13}\text{C}$ spin-spin coupling is barely visible in the 1D ^{19}F spectrum of $[\text{P}(\text{SMA}_{13}\text{-stat-MOTMA}_1)]^+[\text{TFPhB}]^-$ shown in Figure 2. Figure 3 shows a magnified version of this spectrum. The doublet expected for coupling between adjacent ^{13}C and ^{19}F nuclei is observed and is shifted

relative to the primary peak. The shift of the center of the peak ($\delta^{19\text{F}} = -0.13$ ppm) and the one-bond spin-spin coupling constant ($^1J_{\text{F-C}} = 272$ Hz) are consistent with the literature [55, 56]. This phenomenon, however, cannot account for the minor peak observed at -63 ppm in the 1D $^{19\text{F}}$ NMR spectrum of the $[\text{P}(\text{SMA}_{13}\text{-stat-MOTMA}_1)\text{-PBzMA}_{40}]^+[\text{TFPhB}]^-$ nanoparticles shown in Figure 2. This is because this peak is a singlet rather than a doublet and its peak shift is -1 ppm, rather than -0.1 ppm. Therefore, spin-spin coupling can also be discounted as an explanation for the minor peak observed at -63 ppm in Figure 2.

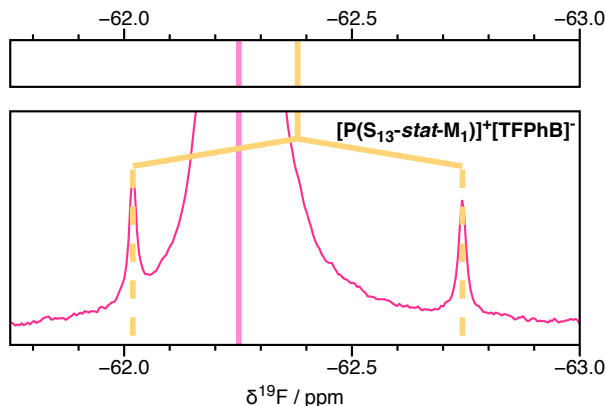


Figure 3: 1D $^{19\text{F}}$ NMR spectrum of a solution of $[\text{P}(\text{SMA}_{13}\text{-stat-MOTMA}_1)]^+[\text{TFPhB}]^-$ copolymer dissolved in *n*-dodecane (7 mol m^{-3}). Spin-spin coupling between the $^{19\text{F}}$ and $^{13\text{C}}$ nuclei is clearly detected for this system.

To determine the connectivity between the $^{19\text{F}}$ and $^{13\text{C}}$ nuclei, $^{19\text{F}}\text{-}^{13\text{C}}$ HSQC NMR experiments were performed. These were devised to investigate whether the minor peak in the $^{19\text{F}}$ NMR spectrum was due to an impurity with a $^{19\text{F}}$ chemical shift similar to that of $[\text{TFPhB}]^-$ or whether it was associated with the $[\text{TFPhB}]^-$ anion. The 2D spectrum, with projected 1D $^{19\text{F}}$ and $^{13\text{C}}$ spectra, is shown in Figure S2. The projected $^{19\text{F}}$ spectrum is almost identical to the previously shown 1D spectrum (Figure 2), and the peak in the projected $^{13\text{C}}$ NMR spectrum agrees with $^{13\text{C}}$ NMR data previously reported for $\text{Na}^+[\text{TFPhB}]^-$ [55, 56]. The minor $^{19\text{F}}$ peak at approximately -63 ppm is also shifted slightly in the $^{13\text{C}}$ axis compared to the major peak at -62 ppm. Given that the two peaks appear at essentially the same chemical shifts (both in the $^{19\text{F}}$ and $^{13\text{C}}$ axes) suggests that is unlikely to be due to an impurity. The imperfect overlap between the two peaks indicates that the minor one has subtly different $^{13\text{C}}$ and $^{19\text{F}}$ environments. This is consistent with our hypothesis that the minor peak in fact arises from a population of free anions.

3.2. Comparison of NMR spectroscopy of fully and partly ionic macromolecules and nanoparticles

Having demonstrated that the two peaks observed in the $^{19\text{F}}$ NMR spectra arise from two different local environments for the $[\text{TFPhB}]^-$ anion, we now study the interaction of this counterion with cationic diblock copolymer nanoparticles, where either some or all of the steric stabilizer chains contain cationic repeat units. In the fully ionic case, PISA syntheses were conducted using solely the $[\text{P}(\text{SMA}_{13}\text{-stat-MOTMA}_1)]^+$ copolymer; in the partly ionic case, a binary mixture of $[\text{P}(\text{SMA}_{13}\text{-stat-MOTMA}_1)]^+$ copolymer and PSMA_{13} homopolymer were used as steric stabilizers. Quantitative 1D $^{19\text{F}}$ NMR spectroscopy enables the proportions of the spectroscopically-distinguishable anionic species to be determined, and diffusion NMR measurements provide important information about their solvodynamic size. Importantly, diffusion NMR analyses do not require any *a priori* knowledge of the local environment of these anionic species.

3.2.1. Solutions of $[\text{P}(\text{SMA}_{13}\text{-stat-MOTMA}_1)]^+$ and PSMA_{13} polymers dissolved in *n*-dodecane

^1H NMR measurements were conducted on $[\text{P}(\text{SMA}_{13}\text{-stat-MOTMA}_1)]^+[\text{TFPhB}]^-$ copolymer dissolved in *n*-dodecane as well as a binary mixture of 10% $[\text{P}(\text{SMA}_{13}\text{-stat-MOTMA}_1)]^+[\text{TFPhB}]^-$ copolymer and 90%

165 PSMA₁₃ homopolymer also dissolved in *n*-dodecane. Partial spectra of the aromatic regions of two polymer solutions are shown in Figure S3. There are two aromatic proton peaks for the [TFPhB][−] anion assigned to the 2, 4 and 6 positions, while the remaining aromatic peaks are attributed to the dithiobenzoate-based RAFT chain-ends. By integrating these peaks, we calculate that the ratio of [TFPhB][−] to dithiobenzoate is 0.96 for the [P(SMA₁₃-*stat*-MOTMA₁)]⁺ [TFPhB][−] copolymer solution and is 0.08 for the binary mixture of [P(SMA₁₃-*stat*-MOTMA₁)]⁺ [TFPhB][−] copolymer and PSMA₁₃ homopolymer. These values correspond to the stoichiometric ratio expected for a monovalent electrolyte.

175 ¹H diffusion NMR measurements conducted on these solutions show that the proton diffusion coefficients for peaks assigned to the dithiobenzoate chain-ends and the [TFPhB][−] anion have different self-diffusion coefficients (*D*). For comparison, ¹⁹F diffusion NMR experiments were also performed. A modified Stokes–Einstein equation was used to calculate the sphere-equivalent solvodynamic radii for these two species. We use an expression derived by Chen and Chen, which replaces the 1/6 prefactor in the Stokes–Einstein equation (stick boundary condition) with a 1/*c* prefactor that depends on the relative radii of the solvent molecules and the solvodynamic radius of the diffusing species [57, 58]. The structure of long-chain *n*-alkanes, such as *n*-dodecane, is akin to that of a polymer melt [59, 60], so the radius of gyration (*R_g*) of *n*-dodecane calculated from neutron scattering (4.5 Å) was used as the solvent radius [59]. The Stokes–Einstein equation [61, 62] was used to calculate an initial solvodynamic radius, which was used as input for the equation reported by Chen and Chen [57, 58]. This calculation was iterated until the radius converged to within ±0.1 Å. A summary of the diffusion coefficients (*D*) and solvodynamic radii (*r*) determined for the two polymer solutions using ¹H and ¹⁹F diffusion NMR is shown in Table 1. The fit *R_g* of [P(SMA₁₃-*stat*-MOTMA₁)]⁺ [MOTMA][−] polymer from SAXS data on nanoparticles prepared using this polymer as a steric stabilizer is 13.8 Å [48]. The sphere-equivalent radius is ($\sqrt{5/3} \cdot R_g$) [63], and this polymer, therefore, has a mean radius of 17.9 Å. This agrees well with the solvodynamic radii shown in Table 1. The two radii calculated for the highly-fluorinated anion are consistent for the ¹H and ¹⁹F nuclei and are greater than that for the dithiobenzoate chain ends of the polymer by 4–5 Å. Thus the anion is predominantly tightly bound to the macromolecular cation. However, the majority of the PSMA polymers are not associated with the anion. The diffusion coefficient for the macromolecular cation is that expected for the polymer chains alone, rather than that of the ion pair complex.

Table 1: Summary of ¹H and ¹⁹F NMR diffusion coefficients (*D*) in *n*-dodecane obtained for solutions of [P(SMA₁₃-*stat*-MOTMA₁)]⁺ [TFPhB][−] copolymer and a binary ionic-nonionic mixture of (0.10)[P(SMA₁₃-*stat*-MOTMA₁)]⁺ [TFPhB][−]—(0.90)[PSMA₁₃].

| Solution | (CDB) | | ([TFPhB] [−]) | |
|--|--|--------------|--|--------------|
| | <i>D</i> / (10 ^{−11} m ² s ^{−1}) | <i>r</i> / Å | <i>D</i> / (10 ^{−11} m ² s ^{−1}) | <i>r</i> / Å |
| Fully ionic (¹ H) | 8.57 | 18.9 | 6.96 | 23.1 |
| Fully ionic (¹⁹ F) | — | — | 6.85 | 23.5 |
| Binary ionic-nonionic (¹ H) | 8.78 | 18.5 | 6.77 | 23.7 |
| Binary ionic-nonionic (¹⁹ F) | — | — | 6.63 | 24.2 |

3.2.2. Dispersions of sterically-stabilized nanoparticles

195 ¹⁹F NMR spectra were measured for two different dispersions of sterically-stabilized diblock copolymer nanoparticles. In one case, the steric stabilizer of the nanoparticles consists of solely cationic [P(SMA₁₃-*stat*-MOTMA₁)]⁺ [TFPhB][−] copolymer, and in the other case, the stabilizer layer consists of a binary mixture of 10% [P(SMA₁₃-*stat*-MOTMA₁)]⁺ [TFPhB][−] copolymer and 90% PSMA₁₃ homopolymer. The 1D ¹⁹F NMR spectra of both types of nanoparticles are shown in Figure 4. The nanoparticle concentrations were identical, which means that the peak integrals can be directly compared. Each spectrum can be fit as a sum of four peaks. There are two broad peaks that form the major peak at around −62 ppm, and also two minor peaks. According to the diffusion NMR data on these same dispersions, these peaks have different

self-diffusion coefficients. It is only the two most intense peaks (the major peak at -63 ppm and the most intense minor peak at -63 ppm) that can be determined from the analysis of the diffusion NMR data. These two peaks in the diffusion axis of the DOSY plots are as easily resolved as the peaks in the 1D spectra in Figure 4. This confirms that these are two entirely distinct environments. The intermediate and least intense peak is too broad in the diffusion NMR data to be determined with certainty. The major peak at -62 ppm corresponds to the slowest-diffusing species, and the other most intense minor peak (at -62 ppm) corresponds to a fast diffusing species, with a self-diffusion coefficient commensurate to a small molecule. A summary of the respective self-diffusion coefficients and corresponding solvodynamic radii is provided in Table 2.

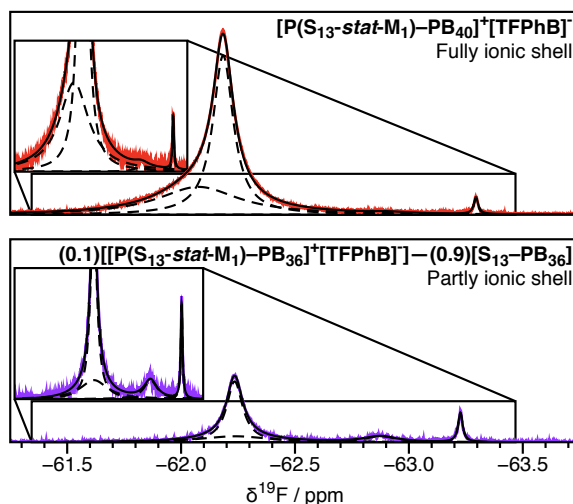


Figure 4: 1D ^{19}F NMR spectra recorded for dispersions of nanoparticles with a fully ionic shell ($[\text{P}(\text{SMA}_{13}\text{-stat-MOTMA}_1)\text{-PBzMA}_{40}]^+[\text{TFPhB}]^-$) (top) and of nanoparticles with a partly ionic shell ($(0.1)[\text{P}(\text{SMA}_{13}\text{-stat-MOTMA}_1)\text{-PBzMA}_{36}]^+[\text{TFPhB}]^- - (0.9)[\text{PSMA}_{13}\text{-PBzMA}_{36}]$) (bottom) ($\phi = 0.08$). Both spectra consist of a single major peak and two minor peaks.

Table 2: Summary of characterizations of fully ionic shell ($[\text{P}(\text{SMA}_{13}\text{-stat-MOTMA}_1)\text{-PBzMA}_{40}]^+[\text{TFPhB}]^-$) and partly ionic shell ($(0.1)[\text{P}(\text{SMA}_{13}\text{-stat-MOTMA}_1)\text{-PBzMA}_{36}]^+[\text{TFPhB}]^- - (0.9)[\text{PSMA}_{13}\text{-PBzMA}_{36}]$) nanoparticles by ^{19}F NMR.

| $\delta \text{ }^{19}\text{F} / \text{ppm}$ | $D / (10^{-11} \text{ m}^2 \text{ s}^{-1})$ | $r / \text{\AA}$ | Proportion of total intensity / % |
|---|---|------------------|-----------------------------------|
| Fully ionic shell | | | |
| -62.1 | 2.52 | 62.8 | 97.7 |
| -62.9 | — | — | 1.0 |
| -63.3 | 33.5 | 6.3 | 1.3 |
| Partly ionic shell | | | |
| -62.2 | 2.29 | 69.1 | 80.7 |
| -62.8 | — | — | 7.7 |
| -63.2 | 32.2 | 6.4 | 11.6 |

The self-diffusion coefficient for anions that are bound to the cationic nanoparticles will be substantially lower than that for free anions in solution. The diffusion NMR data for the nanoparticle systems support

the existence of strong anion binding (Table 2). Both systems have major peaks whose diffusion coefficients and corresponding solvodynamic radii are commensurate with the dimensions of a nanoparticle. The solvodynamic radius from DLS is 100 Å for the fully ionic shell particles and 145 Å for the partly ionic shell nanoparticles. The most intense of the minor peaks has a diffusion coefficient similar to that expected for free ions. The solvodynamic radius of the free [TFPhB]⁻ anions (6.3–6.4 Å) compares favorably to the molecular size of this anion calculated by summing volume increments (4.9 Å [64]) or determined from diffusion NMR measurements conducted in non-aliphatic hydrocarbon solvents (6 Å [33]). These diffusion coefficients and solvodynamic radii enable us to assign the environment of the two peaks in the 1D NMR spectra with confidence.

The electrophoretic mobility of the fully cationic shell nanoparticles is known to be lower than that of nanoparticles prepared using a binary mixture of nonionic and cationic steric stabilizers [18, 48]. Moreover from the data presented here, the proportion of counterions in distinct environments (as judged by ¹⁹F NMR spectroscopy) differs for the two systems (Figure 4 and Table 2). It seems that a minor population of fast-diffusing nuclei (with a ¹⁹F NMR chemical shift that differs by ~ 1 ppm compared to the major population) arises from highly-fluorinated anions that have become fully dissociated from the interface of the cationic nanoparticles, which in turn leads to a higher electrophoretic mobility.

4. Conclusions

In summary, NMR spectroscopy using ¹H, ¹³C, and ¹⁹F nuclei can be used to study the degree of dissociation of the weakly-coordinating anion, [tetrakis-[3,5-bis(trifluoromethyl)phenyl]borate]⁻ ([TFPhB]⁻), in a non-polar solvent (*n*-dodecane). When this highly-fluorinated anionic counterion is associated with a cationic, oil-soluble copolymer, only a single fluorine environment is detected with a diffusion coefficient (and associated solvodynamic radius) corresponding to that expected for ion pairs. However, when this anion is associated with cationic, sterically-stabilized diblock copolymer nanoparticles, multiple fluorine environments can be observed. Importantly, one of these environments has a diffusion coefficient corresponding to that expected of the free anion. We believe that this is the first direct spectroscopic evidence for such free ions in an aliphatic non-polar solvent. Only ion pairs and higher-number aggregates have been reported in such solvents previously [26, 27, 34].

These observations address a currently unexplained phenomenon recently reported for charged shell nanoparticles in a salt-free medium [18, 48]. The electrophoretic mobility of charged shell nanoparticles with a small proportion (≲ 30%) of steric stabilizer chains containing cationic moieties has a greater magnitude than that of charged shell nanoparticles with all steric stabilizer chains containing an ionic group. Here, we show that a significantly higher proportion of free anions are detected when the cationic comonomer is only incorporated into a minor fraction (10%) of the steric stabilizer chains of these diblock copolymer nanoparticles. These two findings are consistent. When the magnitude of electrophoretic mobility of the charged nanoparticles is greater, the proportion of free ions is also greater. No existing electrokinetic theories of soft charged particles or salt-free charged particles can explain these observations [65–69]. The ability to quantify the proportion of free ions and ion pairs at the colloidal interface should provide valuable experimental data to enable this situation to be addressed.

Acknowledgements

SPA and GNS acknowledge the ERC for a five-year Advanced Investigator grant (PISA 320372) and EPSRC (EP/J007846) for funding GNS. SPA is the recipient of a four-year EPSRC Established Career Particle Technology Fellowship (EP/R003009/1). Dr. G. Facey (University of Ottawa, Canada) is acknowledged for an informative scientific discussion and his measurements of isotope effects detailed in his blog post “Isotope Effects and the ¹⁹F - ¹³C HMQC Spectrum of Trifluoroacetic Acid” (<http://u-of-o-nmr-facility.blogspot.com/2012/10/isotope-effects-and-19-f-13-c-hmqc.html>).

References

- [1] I. D. Morrison, Electrical charges in nonaqueous media, *Colloids Surf. A: Physicochem. Eng. Aspects* 71 (1) (1993) 1–37. doi:10.1016/0927-7757(93)80026-B.
- [2] G. N. Smith, J. Eastoe, Controlling colloid charge in nonpolar liquids with surfactants, *Phys. Chem. Chem. Phys.* 15 (2) (2013) 424–439. doi:10.1039/c2cp42625k.
- [3] R. Moritz, G. Zardalidis, H.-J. Butt, M. Wagner, K. Müllen, G. Floudas, Ion size approaching the Bjerrum length in solvents of low polarity by dendritic encapsulation, *Macromolecules* 47 (1) (2014) 191–196. doi:10.1021/ma402137x.
- [4] A. Klinkenberg, J. L. van der Minne (Eds.), *Electrostatics in the Petroleum Industry: The Prevention of Explosion Hazards*, Elsevier, London, 1958.
- [5] V. Novotny, Applications of nonaqueous colloids, *Colloids Surf.* 24 (4) (1987) 361–375. doi:10.1016/0166-6622(87)80241-X.
- [6] S. H. Strauss, The search for larger and more weakly coordinating anions, *Chem. Rev.* 93 (3) (1993) 927–942. doi:10.1021/cr00019a005.
- [7] B. Comiskey, J. D. Albert, H. Yoshizawa, J. Jacobson, An electrophoretic ink for all-printed reflective electronic displays, *Nature* 394 (6690) (1998) 253–255. doi:10.1038/28349.
- [8] E. Y.-X. Chen, T. J. Marks, Cocatalysts for metal-catalyzed olefin polymerization: Activators, activation processes, and structure–activity relationships, *Chem. Rev.* 100 (4) (2000) 1391–1434. doi:10.1021/cr980462j.
- [9] R. E. LaPointe, G. R. Roof, K. A. Abboud, J. Klosin, New family of weakly coordinating anions, *J. Am. Chem. Soc.* 122 (39) (2000) 9560–9561. doi:10.1021/ja002664e.
- [10] T. Hao, Electrorheological fluids, *Adv. Mater.* 13 (24) (2001) 1847–1857. doi:10.1002/1521-4095(200112)13:24<1847::AID-ADMA1847>3.0.CO;2-A.
- [11] J. Heikenfeld, P. Drzaic, J.-S. Yeo, T. Koch, Review paper: A critical review of the present and future prospects for electronic paper, *J. Soc. Info. Display* 19 (2) (2011) 129–156. doi:10.1889/JSID19.2.129.
- [12] A. P. Abbott, T. A. Claxton, J. Fawcett, J. C. Harper, Tetrakis(decyl)ammonium tetraphenylborate: a novel electrolyte for non-polar media, *J. Chem. Soc., Faraday Trans.* 92 (10) (1996) 1747–1749. doi:10.1039/FT9969201747.
- [13] A. P. Abbott, G. A. Griffith, J. C. Harper, Conductivity of long chain quaternary ammonium electrolytes in cyclohexane, *J. Chem. Soc., Faraday Trans.* 93 (4) (1997) 577–582. doi:10.1039/A607230E.
- [14] G. Hussain, A. Robinson, P. Bartlett, Charge generation in low-polarity solvents: Poly(ionic liquid)-functionalized particles, *Langmuir* 29 (13) (2013) 4204–4213. doi:10.1021/la3049086.
- [15] R. M. Fuoss, C. A. Kraus, Properties of electrolytic solutions. IV. The conductance minimum and the formation of triple ions due to the action of coulomb forces, *J. Am. Chem. Soc.* 55 (6) (1933) 2387–2399. doi:10.1021/ja01333a026.
- [16] D. A. J. Gillespie, J. E. Hallett, O. Elujoba, A. F. Che Hamzah, R. M. Richardson, P. Bartlett, Counterion condensation on spheres in the salt-free limit, *Soft Matter* 10 (4) (2014) 566–577. doi:10.1039/C3SM52563E.
- [17] A. V. Delgado, F. Carrique, R. Roa, E. Ruiz-Reina, Recent developments in electrokinetics of salt-free concentrated suspensions, *Curr. Opin. Colloid Interface Sci.* 24 (2016) 32–43. doi:10.1016/j.cocis.2016.06.004.
- [18] G. N. Smith, L. L. E. Mears, S. E. Rogers, S. P. Armes, Synthesis and electrokinetics of cationic spherical nanoparticles in salt-free non-polar media, *Chem. Sci.* 9 (2018) 922–934. doi:10.1039/C7SC03334F.
- [19] J. Lee, Z.-L. Zhou, G. Alas, S. H. Behrens, Mechanisms of particle charging by surfactants in nonpolar dispersions, *Langmuir* 31 (44) (2015) 11989–11999. doi:10.1021/acs.langmuir.5b02875.
- [20] E. L. Michor, B. S. Ponto, J. C. Berg, Effects of reverse micellar structure on the particle charging capabilities of the Span surfactant series, *Langmuir* 32 (40) (2016) 10328–10333. doi:10.1021/acs.langmuir.6b02959.
- [21] N. Hiroshi, T. Naoko, Y. Masaji, S. Takaaki, K. Hiroshi, Tetrakis[3,5-bis(trifluoromethyl)phenyl]borate. Highly lipophilic stable anionic agent for solvent-extraction of cations, *Bull. Chem. Soc. Japan* 57 (9) (1984) 2600–2604. doi:10.1246/bcsj.57.2600.
- [22] T. Ono, M. Ohta, K. Sada, Ionic polymers act as polyelectrolytes in nonpolar media, *ACS Macro Lett.* 1 (11) (2012) 1270–1273. doi:10.1021/mz3002879.
- [23] P. S. Pregosin, E. Martínez-Viviente, P. G. A. Kumar, Diffusion and NOE NMR spectroscopy. Applications to problems related to coordination chemistry and homogeneous catalysis, *Dalton Trans.* 21 (2003) 4007–4014. doi:10.1039/B305046G.
- [24] P. S. Pregosin, P. G. A. Kumar, I. Fernández, Pulsed gradient spin–echo (PGSE) diffusion and ^1H , ^{19}F heteronuclear overhauser spectroscopy (hocsy) nmr methods in inorganic and organometallic chemistry: Something old and something new, *Chem. Rev.* 105 (8) (2005) 2977–2998. doi:10.1021/cr0406716.
- [25] A. Macchioni, Ion pairing in transition-metal organometallic chemistry, *Chem. Rev.* 105 (6) (2005) 2039–2074. doi:10.1021/cr0300439.
- [26] L. Rocchigiani, C. Zuccaccia, D. Zuccaccia, A. Macchioni, Self-aggregation tendency of zirconocenium ion pairs which model polymer-chain-carrying species in aromatic and aliphatic solvents with low polarity, *Chem. Eur. J.* 14 (22) (2008) 6589–6592. doi:10.1002/chem.200800818.
- [27] L. Rocchigiani, G. Bellachioma, G. Ciancaleoni, A. Macchioni, D. Zuccaccia, C. Zuccaccia, Synthesis, characterization, interionic structure, and self-aggregation tendency of zirconaaziridinium salts bearing long alkyl chains, *Organometallics* 30 (1) (2011) 100–114. doi:10.1021/om100827z.
- [28] P. Griffiths, P. Stilbs, NMR self-diffusion studies of polymeric surfactants, *Curr. Opin. Colloid Interface Sci.* 7 (3) (2002) 249–252. doi:10.1016/S1359-0294(02)00042-0.
- [29] P. C. Griffiths, A. Y. F. Cheung, J. A. Davies, A. Paul, C. N. Tipples, A. L. Winnington, Probing interactions within complex colloidal systems using PGSE-NMR, *Magn. Reson. Chem.* 40 (13) (2002) S40–S50. doi:10.1002/mrc.1131.

- [30] W. Li, H. Chung, C. Daeffler, J. A. Johnson, R. H. Grubbs, Application of ^1H DOSY for facile measurement of polymer molecular weights, *Macromolecules* 45 (24) (2012) 9595–9603. doi:10.1021/ma301666x.
- [31] P. Groves, Diffusion ordered spectroscopy (DOSY) as applied to polymers, *Polym. Chem.* 8 (2017) 6700–6708. doi:10.1039/C7PY01577A.
- 325 [32] K. Gu, J. Onorato, S. S. Xiao, C. K. Luscombe, Y.-L. Loo, Determination of the molecular weight of conjugated polymers with diffusion-ordered NMR spectroscopy, *Chem. Mater.* 30 (3) (2018) 570–576. doi:10.1021/acs.chemmater.7b05063.
- [33] G. Ciancaleoni, C. Zuccaccia, D. Zuccaccia, A. Macchioni, Combining diffusion NMR and conductometric measurements to evaluate the hydrodynamic volume of ions and ion pairs, *Organometallics* 26 (15) (2007) 3624–3626. doi:10.1021/om700415f.
- 330 [34] B. Endeward, P. Brant, R. D. Nielsen, M. Bernardo, K. Zick, H. Thomann, Aggregation of borate salts in hydrocarbon solvents, *J. Phys. Chem. C* 112 (21) (2008) 7818–7828. doi:10.1021/jp710981g.
- [35] S. L. Canning, G. N. Smith, S. P. Armes, A critical appraisal of RAFT-mediated polymerization-induced self-assembly, *Macromolecules* 49 (6) (2016) 1985–2001. doi:10.1021/acs.macromol.5b02602.
- [36] R. Sánchez, P. Bartlett, Synthesis of charged particles in an ultra-low dielectric solvent, *Soft Matter* 7 (3) (2011) 887–890. doi:10.1039/C0SM01454K.
- 335 [37] G. N. Smith, J. E. Hallett, J. Eastoe, Celebrating *Soft Matter*'s 10th Anniversary: Influencing the charge of poly(methyl methacrylate) latexes in nonpolar solvents, *Soft Matter* 11 (41) (2015) 8029–8041. doi:10.1039/C5SM01190F.
- [38] R. J. Pugh, T. Matsunaga, F. M. Fowkes, The dispersibility and stability of carbon black in media of low dielectric constant. 1. Electrostatic and steric contributions to colloidal stability, *Colloids Surf.* 7 (3) (1983) 183–207. doi:10.1016/0166-6622(83)80046-8.
- 340 [39] R. Pugh, F. Fowkes, The dispersibility and stability of coal particles in hydrocarbon media with a polyisobutene succinamide dispersing agent, *Colloids Surf.* 11 (3) (1984) 423–427. doi:10.1016/0166-6622(84)80295-4.
- [40] J. J. McDermott, Electrostatic stability of colloidal dispersions in nonpolar media. URL <https://weitzlab.seas.harvard.edu/research/current/joseph-j-mcdermott>
- 345 [41] J. J. McDermott, Salting-out of dilute electrostatic carbon dispersions. URL <https://weitzlab.seas.harvard.edu/research/current/joseph-j-mcdermott>
- [42] B. Derjaguin, A theory of interaction of particles in presence of electric double-layers and the stability of lyophobic colloids and disperse systems, *Acta Physicochim. URSS* 10 (1939) 333–346.
- [43] B. Derjaguin, L. D. Landau, Theory of the stability of strongly charged lyophobic sols and of the adhesion of strongly charged particles in solutions of electrolytes, *Acta Physicochim. URSS* 14 (1941) 633–662.
- 350 [44] E. J. W. Verwey, J. Th. G. Overbeek, *Theory of Stability of Lyophobic Colloids*, Elsevier, Amsterdam, 1948.
- [45] C. Wohlfarth, Permittivity (dielectric constant) of liquids, in: *CRC Handbook of Chemistry and Physics*, 95th Edition, CRC Press, 2014–2015 (Internet Version), Ch. Permittivity (Dielectric Constant) Of Liquids.
- [46] S. D. Finlayson, P. Bartlett, Non-additivity of pair interactions in charged colloids, *J. Chem. Phys.* 145 (3) (2016) 034905. doi:10.1063/1.4959122.
- 355 [47] G. N. Smith, S. D. Finlayson, S. E. Rogers, P. Bartlett, J. Eastoe, Electrolyte-induced instability of colloidal dispersions in nonpolar solvents, *J. Phys. Chem. Lett.* 8 (19) (2017) 4668–4672. doi:10.1021/acs.jpcllett.7b01685.
- [48] G. N. Smith, S. L. Canning, M. J. Derry, E. R. Jones, T. J. Neal, A. J. Smith, Ionic and nonspherical polymer nanoparticles in nonpolar solvents, *Macromolecules* (2020). doi:10.1021/acs.macromol.0c00121.
- 360 [49] M. Wojdyr, *Fityk*: a general-purpose peak fitting program, *J. Appl. Cryst.* 43 (5 Part 1) (2010) 1126–1128. doi:10.1107/S0021889810030499.
- [50] M. Nilsson, The DOSY Toolbox: A new tool for processing PFG NMR diffusion data, *J. Magn. Reson.* 200 (2) (2009) 296–302. doi:10.1016/j.jmr.2009.07.022.
- [51] N. Bjerrum, Untersuchungen über ionenassoziation. I. Der einfluss der ionenassoziation auf die aktivität der ionen bei mittleren assoziationsgraden., *Kgl. Danske Vidensk. Selsk., Math.-fys. Medd.* 7 (9) (1926) 1–48.
- 365 [52] H. Matsuo, K. J. Walters, K. Teruya, T. Tanaka, G. T. Gassner, S. J. Lippard, Y. Kyogoku, G. Wagner, Identification by NMR spectroscopy of residues at contact surfaces in large, slowly exchanging macromolecular complexes, *J. Am. Chem. Soc.* 121 (42) (1999) 9903–9904. doi:10.1021/ja991881g.
- [53] J. Battiste, R. A. Newmark, Applications of ^{19}F multidimensional NMR, *Prog. Nucl. Magn. Reson. Spectrosc.* 48 (1) (2006) 1–23. doi:10.1016/j.pnmrs.2005.10.002.
- 370 [54] R. K. J. R., T. P. D. P., *Isotopic compositions of the elements 1997 (Technical Report)*, *Pure Appl. Chem.* 70 (1998) 217. doi:10.1351/pac199870010217.
- [55] A. C. Filippou, N. Weidemann, G. Schnakenburg, H. Rohde, A. I. Philippopoulos, Tungsten–lead triple bonds: Syntheses, structures, and coordination chemistry of the plumbidyne complexes *trans*-[x(pme₃)₄ ≡pb(2,6-trip₂c₆h₃)], *Angew. Chem. Int. Ed.* 43 (47) (2004) 6512–6516. doi:10.1002/anie.200461725.
- 375 [56] N. A. Yakelis, R. G. Bergman, Safe preparation and purification of sodium tetrakis[(3,5-trifluoromethyl)phenyl]borate (nabarf₂₄): Reliable and sensitive analysis of water in solutions of fluorinated tetraarylborates, *Organometallics* 24 (14) (2005) 3579–3581. doi:10.1021/om0501428.
- [57] H. C. Chen, S. H. Chen, Diffusion of crown ethers in alcohols, *J. Phys. Chem.* 88 (21) (1984) 5118–5121. doi:10.1021/j150665a063.
- 380 [58] A. Macchioni, G. Ciancaleoni, C. Zuccaccia, D. Zuccaccia, Determining accurate molecular sizes in solution through NMR diffusion spectroscopy, *Chem. Soc. Rev.* 37 (3) (2008) 479–489. doi:10.1039/B615067P.
- [59] F. Goodsaid-Zalduondo, D. M. Engelman, Conformation of liquid *N*-alkanes, *Biophys. J.* 35 (3) (1981) 587–594. doi:10.1016/S0006-3495(81)84814-X.
- 385 [60] L. Arleth, J. S. Pedersen, Scattering vector dependence of the small-angle scattering from mixtures of hydrogenated and

deuterated organic solvents, *J. Appl. Cryst.* 33 (3-1) (2000) 650–652. doi:10.1107/S0021889899012789.

- [61] A. Einstein, Eine neue bestimmung der moleküldimensionen, *Ann. Phys.* 324 (2) (1906) 289–306. doi:10.1002/andp.19063240204.
- [62] A. Einstein, Berichtigung zu meiner Arbeit: „Eine neue bestimmung der moleküldimensione“, *Ann. Phys.* 339 (3) (1911) 591–592. doi:10.1002/andp.19113390313.
- 390 [63] B. Hammouda, Probing nanoscale structures—The SANS toolbox.
URL http://www.ncnr.nist.gov/staff/hammouda/the_SANS_toolbox.pdf
- [64] J. T. Edward, Molecular volumes and the Stokes–Einstein equation, *J. Chem. Ed.* 47 (4) (1970) 261–270. doi:10.1021/ed047p261.
- 395 [65] H. Ohshima, Electrophoretic mobility of a spherical colloidal particle in a salt-free medium, *J. Colloid Interface Sci.* 248 (2) (2002) 499–503. doi:10.1006/jcis.2002.8232.
- [66] H. Ohshima, Electrokinetic phenomena in a dilute suspension of spherical colloidal particles in a salt-free medium, *Colloids Surf. A: Physicochem. Eng. Aspects* 222 (1) (2003) 207–211. doi:10.1016/S0927-7757(03)00225-5.
- [67] H. Ohshima, Numerical calculation of the electrophoretic mobility of a spherical particle in a salt-free medium, *J. Colloid Interface Sci.* 262 (1) (2003) 294–297. doi:10.1016/S0021-9797(03)00190-5.
- 400 [68] H. Ohshima, Electrophoretic mobility of a soft particle in a salt-free medium, *J. Colloid Interface Sci.* 269 (1) (2004) 255–258. doi:10.1016/S0021-9797(03)00600-3.
- [69] H. Ohshima, Erratum to “Electrophoretic mobility of a soft particle in a salt-free medium”: [*J. Colloid Interface Sci.* 269 (2004) 255–258], *J. Colloid Interface Sci.* 272 (2) (2004) 503. doi:10.1016/j.jcis.2003.12.063.

